THE INSTITUTE FOR SYSTEMS RESEARCH

ISR TECHNICAL REPORT 2008-24

# Coordination in Networked Mechanical Systems

Shah, Rajiv P., Advisor: Chopra, Nikhil

**UNDERGRADUATE REPORT**

# COORDINATION IN NETWORKED MECHANICAL SYSTEMS

**Rajiv P. Shah**

**Faculty Mentor: Dr. Nikhil Chopra**

**Research Experiences for Undergraduates Program**

**Institute for Systems Research, University of Maryland**

**August 7, 2008**

## Table of Contents

## Abstract

The goal of this summer research was to find a way to control mechanical systems over unreliable communication networks. These systems become unstable due to time delay in the communication port. Using wave scattering theory, we solved the problem of time delay in a bilateral teleoperation and controlled network systems. For both bilateral teleoperation and controlled network systems, we created theoretical simulations in MATLAB for three cases: in absence of time delay, in presence of time delay, and in the case of time delay compensation. In the lab, we tested the theoretical simulation design of controlled network system on a simple servo system for all three cases. We controlled the servo system by implementing the wave scattering transformation to solve the problem of time delay. We recorded the steady state error for various time delays and concluded that as time delay increased, the steady state error in system's response increased as well.

## Introduction

### Bilateral Teleoperation

Telerobotics is the body of science and technology that bridges human control and purely autonomous machines. Telerobotics is a merging point of modern developments in robotics, control theory, cognitive science, machine design, and computer science.[1] Some of the applications of bilateral teleoperation are manipulating space robots and undersea vehicles from ground, handling dangerous materials, and helping doctors in surgery and telemedicine.[3]

In teleoperation, a human operator from a remote location conducts a task in remote environment through master and slave manipulators. Therefore, being able to provide contact force information from the slave back to the human operator can improve task performance. Although this information can be obtained from visual displays, it is more useful and accurate if provided directly by reflecting the measured force back to the master system. This contact force is thus experienced by the human operator over a great distance, and hence the teleoperator is bilaterally controlled.[2] A teleoperation is composed of five parts: human operator, master system, communication, slave system and environment. A master system is directly controlled by the human operator and a slave system is located in the environment to perform work. The basic diagram of teleoperation is shown in figure 1.


**Figure 1. Block diagram representation of bilateral teleoperation.**

As shown in figure 1, a human operator sends a velocity command ($V_{md}$) to the master. The master then sends a velocity command ($V_m$) to the slave through the communication port. When there is a time delay in the communication port, the slave system receives a delayed velocity command ($V_{sd}$). The slave works in the environment by giving a velocity ($V_s$) and in return, it experiences a force from the environment ($F_e$), which gets transmitted through communication port as $F_s$ through the master that receives $F_m$, and finally the human operator feels the feedback force ($F_h$).

## Controlled Network System

A controlled network system consists of three parts: plant, communication and controller. The basic block diagram of controlled network system is shown in figure 2.

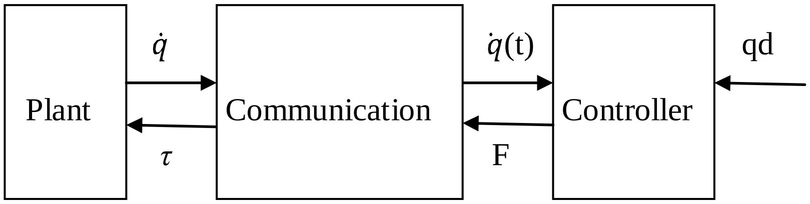


**Figure 2. Block diagram representation of a simple controlled network.**

As shown in figure 2, a controller computes the force F from the velocity command $\dot{q}$ sent by the plant and the desired position (qd) set by the controller. The plant feels the torque $\tau$ and reaches the constant desired position qd with certain velocity $\dot{q}$.

It is very important that the system is passive. A passive master system, communication and slave system ensures the system is overall stable. An n-port is said to be passive if and only if for any independent set of n-port flows, $v_i$ injected into the system, and efforts $F_j$ applied across the system, the following equations holds true.[2]

$$\int_0^\infty F^T(t)v(t)dt \geq 0$$

A concept related to that of passivity is called losslessness. A circuit element is known as lossless if it is passive and if all the energy can be extracted again when a finite amount of energy is put into the element.[5] An n-port is said to be lossless, if and only if:[2]

$$\int_0^\infty F^T(t)v(t)dt = 0$$

Tellegen's theorem yields a very simple proof of the fact that a finite number of passive elements when interconnected yield a passive network.[5] Some examples of passive circuit elements are transformer, transmission line, damping or impedance, stiffness, inertia and gyrator.

## Dynamics of teleoperator system

The dynamics of master and slave in a telerobotic system can be modeled by the following equations:[2]

$$M_m \dot{v}_m = F_h + \tau_m \qquad (1)$$

$$M_s \dot{v}_s = -F_e + \tau_s \qquad (2)$$

where $M_m$ is inertia of master, $v_m$ is velocity of master, $F_h$ is force felt by the human operator, $\tau_m$ is motor torque of master, $M_s$ is inertia of slave, $v_s$ is velocity of slave, $F_e$ is contact force from the environment, and $\tau_s$ is motor torque of slave.

The control system of the bilateral teleoperation system is given by:

$$\tau_m = -B_m v_m - F_m \quad (3)$$

$$\tau_s = -B_{s2} v_s + F_s - \alpha F_e \quad (4)$$

where $B_m$ is damping constant, $F_m$ is desired force for master, $B_{s2}$ is rate of damping constant, and $\alpha$ is force gain constant[2]

In equation (4); $F_s$ is called coordinating torque which is simply

$$F_s = K_s \int (v_{sd} - v_s) dt + B_{s1} (v_{sd} - v_s) \quad (5)$$

where $v_{sd}$ is the desired velocity for slave and $B_{s1}$ is the error damping[2]

When the master system and slave system are far apart, we have to take into consideration time delay. Due to the problem of time delay, we have to perform three separate simulations

1. In the absence of time delay, $F_m = F_s$ and $v_{sd} = v_m$ which results in the following system: [2]

$$M_m \dot{v}_m + B_m v_m = F_h - F_s \quad (6)$$

$$M_m \dot{v}_s + B_{s2} v_s = -F_s + (1 + \alpha) F_e \quad (7)$$

where $F_s = K_s \int (v_m - v_s) dt + B_{s1} (v_m - v_s)$ (8)

2. In the presence of time delay (T), $F_m = F_s(t - T)$ and $v_{sd} = v_m(t - T)$ which results in the following system: [2]

$$M_m \dot{v}_m + B_m v_m = F_h - F_s(t - T) \quad (9)$$

$$M_m \dot{v}_s + B_{s2} v_s = -F_s + (1 + \alpha) F_e \quad (10)$$

where $F_s = K_s \int [v_m(t - T) - v_s] dt + B_{s1} [v_m(t - T) - v_s]$ (11)

3. In the case of solving the time delay problem

The system of equations given by Anderson and Spong for solving the time delay problem is given by[2]

$$F_m(t) = F_s(t-T) + n^2[v_m(t) - v_{sd}(t-T)] \qquad (12)$$

$$v_{sd}(t) = v_m(t-T) + \frac{1}{n^2}[F_m(t-T) - F_s(t)] \qquad (13)$$

Time delay can also be solved by incorporating the wave scattering equations given by Niemeyer and Slotine[1]

$$u_l = \frac{F_m + bv_m}{\sqrt{2b}},\ u_r = \frac{F_s + bv_{sd}}{\sqrt{2b}},\ v_l = \frac{F_m - bv_m}{\sqrt{2b}} \text{ and } v_r = \frac{F_s + bv_{sd}}{\sqrt{2b}} \qquad (14)$$

where b is characteristic impedance of associated wave variables, $u_l$ is input wave to the left port, $u_r$ is input wave to the right port, $v_l$ is output wave to the left port, and $v_r$ is output wave to the right port of the blocks shown in figure 3.

The wave scattering equations can be represented by using the following blocks as shown in figure 3(a) and 3(b).

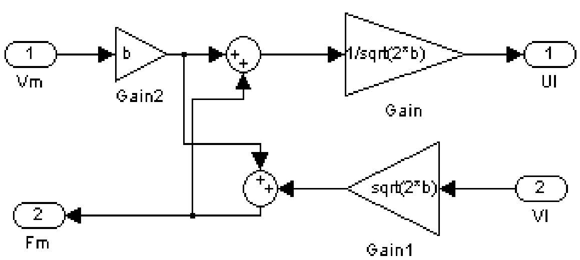


**Figure 3(a). Wave transformation block for master.**

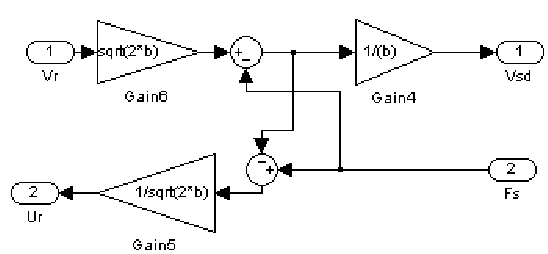


**Figure 3(b). Wave transformation block for slave.**

## Dynamics of controller and plant

Similar to the bilateral teleoperation system, we have to take into consideration time delay in controlled network systems. We have three cases depending on the time delay.

<u>Case 1</u>: In the absence of time delay: the dynamics of controller and plant, assuming no gravity and no force from the environment, is given by:

$$\tau = -M(q)\ddot{q} - C(q,\dot{q})\dot{q} \qquad (15)$$

$$F = k\left\{\int_0^t \dot{q}(t)dt - qd\right\} + B\dot{q}(\mathrm{t}) \qquad (16)$$

where $\tau$ is motor torque of the plant, $\dot{q}$ is desired velocity, F is force applied by the controller, qd is desired position which is a constant, k is proportional gain, and B is derivative gain

Case 2: In the presence of time delay (T), the dynamics of controller and plant is given by:

$$\tau = -M(q)\ddot{q} - C(q,\dot{q})\dot{q}$$

$$F = k\left\{\int_0^t \dot{q}(t-T)dt - qd)\right\} + B\{\dot{q}(t-T)\} \qquad (17)$$

$$\tau = F(t-T) \qquad (18)$$

Case 3: In the case of solving the time delay problem, we use the same priciple of wave scattering theory described by equation 14 and figures 3(a) and 3(b).

## Simulations and results

After knowing the dynamics of bilateral teleoperation and controlled network systems, we created theoretical simulations based on the dynamics of the respective systems. First, we created theoretical simulations of bilateral teleoperation system.

### Bilateral Teleoperation System

We used equations 1- 8 to create a simulation in MATLAB for the bilateral teleoperation system. Figure 4 shows the simulation of a telerobotic system in the absense of time delay.

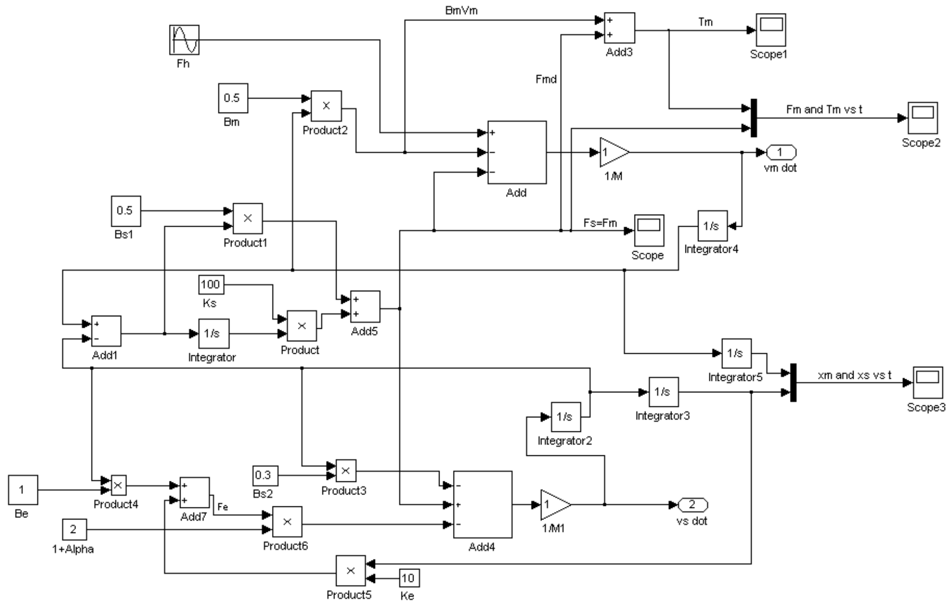


Figure 4. Simulation in the case of no time delay.

Figure 5 represents the output generated by the simulation in figure 4. The position of master and slave is the output.

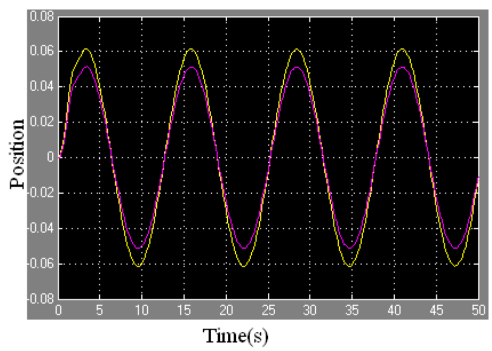


Figure 5. Position of master (yellow) vs. position of slave (red).

In figure 5 we see that in the absence of time delay, the slave system traces the path of the master system when the input provided to the system is a sinusoidal force.

After that, we used equations 9, 10 and 11 to create a theoretical simulation of bilateral teleoperation system when there is a time delay in the communication port.

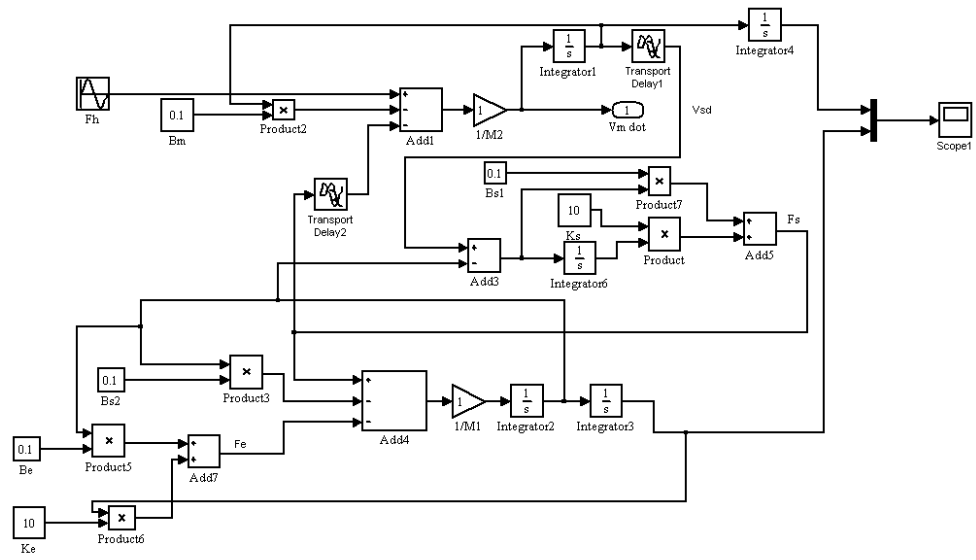


Figure 6. Simulation in the case of time delay.

Figure 7 is the output generated from the simulation in figure 6. Figure 7 is a proof that that when time delay exists, the system becomes unstable. Even a time delay of less than one millionth of seconds can make a system completely unstable.

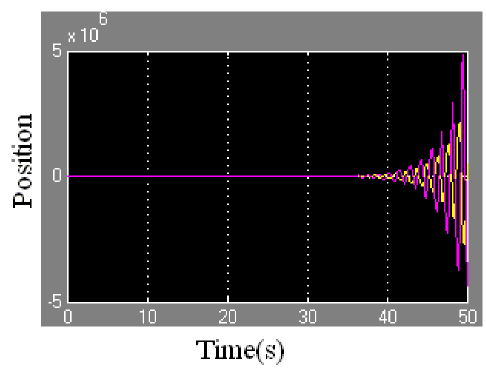


Fig 7. Position of master (yellow) vs. position of slave (red) when time delay=0.1s.

Due to this problem, it is very important to incorporate the wave scattering transformation in our simulation as described in equation 14. There are two ways of solving the time delay problem. One way is to incorporate equations 12 and 13 into our simulation. The other way is to incorporate wave scattering equations into our simulation. Figure 8 is the simulation created using equations 12 and 13 for solving time delay.

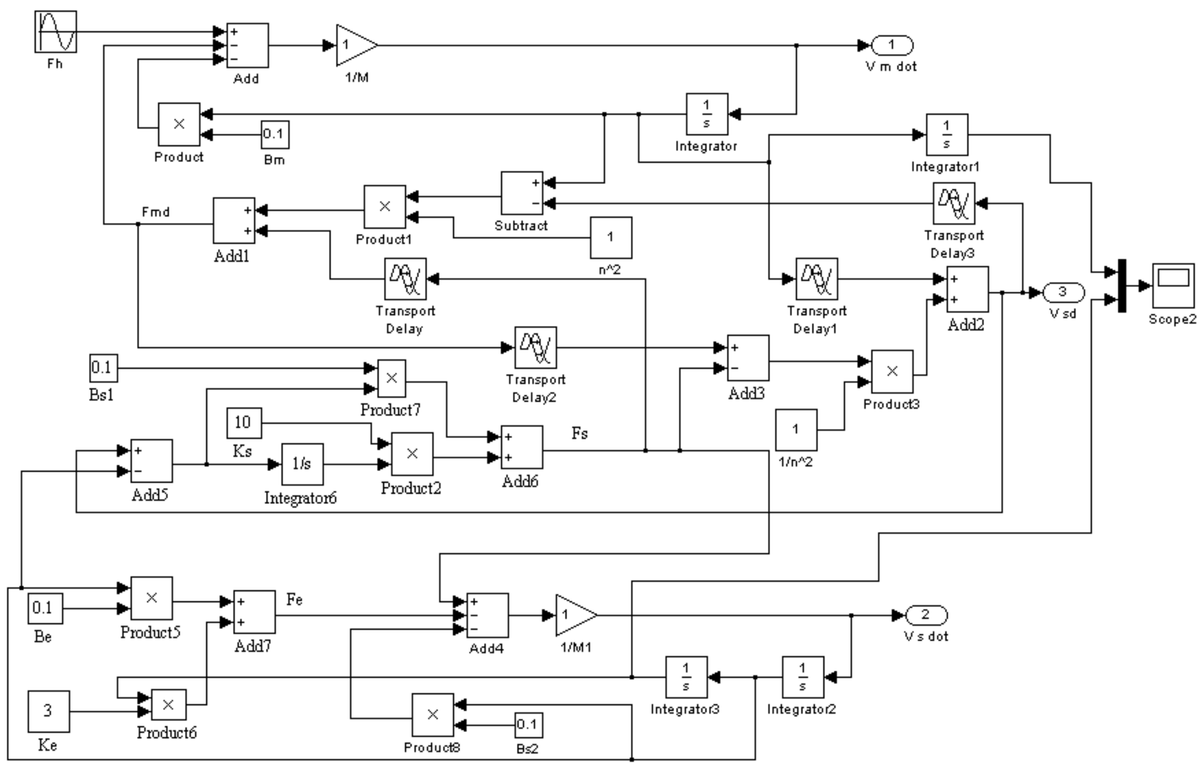


**Figure 8. Simulation created using equations 12 and 13 for solving time delay.**

Similarly, figure 9 is the simulation design that incorporates wave scattering transformation blocks (figure 3(a) and 3(b)) using equation 14 to solve time delay problem.

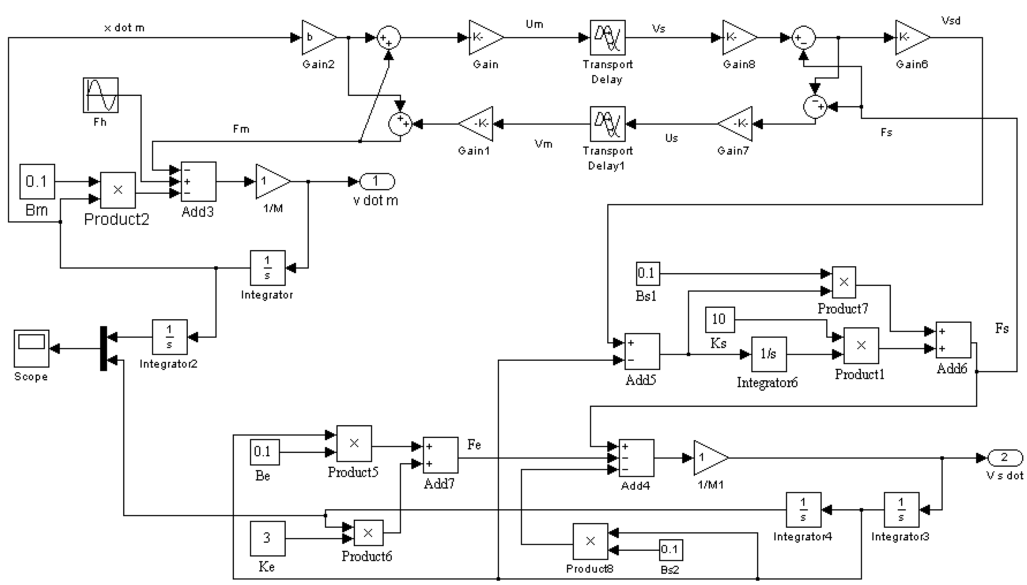


**Figure 9(a). Simulation using wave scattering transformation blocks in the case of compensation of time delay.**

Figure 9(a) can be represented by a simple block diagram as shown in figure 9(b).

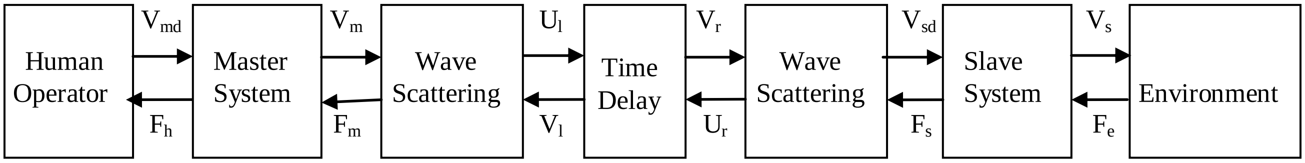


**Figure 9(b). Block diagram with wave scattering which corresponds to the simulation in figure 8(a).**

Both simulations work for time delay less than or equal to 2s and both simulation models in figure 8 and 9(a) give the same output (figure 10). The output of both simulations when time delay is 0.1s and $b=n^2=1$(in equations 12, 13 and 14) is shown in figure 10.

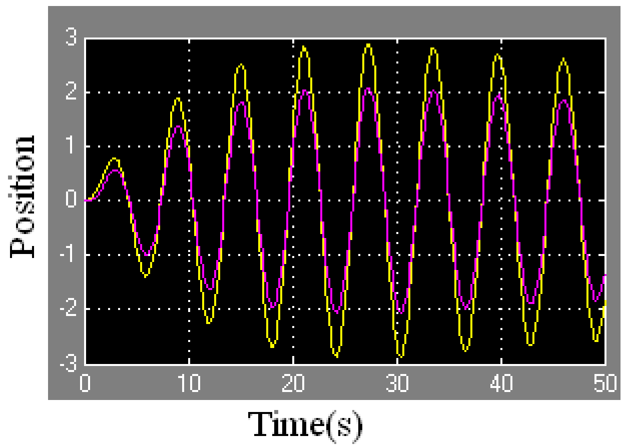


**Figure 10. Position of master (yellow) following the position of slave (red).**

Figure 10 shows the slave system traces the path of the master system. Hence, the wave scattering equations can indeed solve the time delay problem in a bilateral teleoperation system.

## Controlled Network System (Controller and plant)

Similar to the theoretical simulations that we created for bilateral teleoperation system, we created theoretical simulations based upon the dynamics of the controlled network system. We used equations 15 and 16 to create a simulation for controller and plant system in the absence of time delay is shown in figure 11.

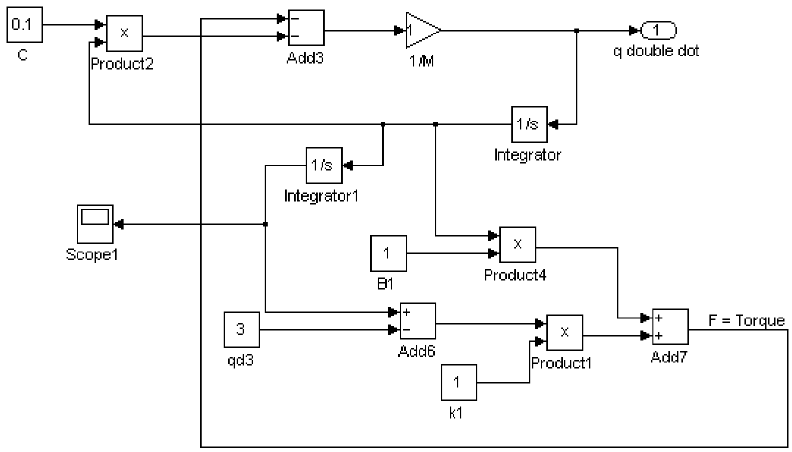


Figure 11. Simulation in the case of no time delay.

The output of the simulation in figure 11 is shown in figure 12. We can see that the position of the plant is controlled as desired. From figure 12, it is obvious that the desired position of the plant is 3 units as set in the simulation design. When we set 3 as our desired input position (qd), we see that the output reaches to 3 units.

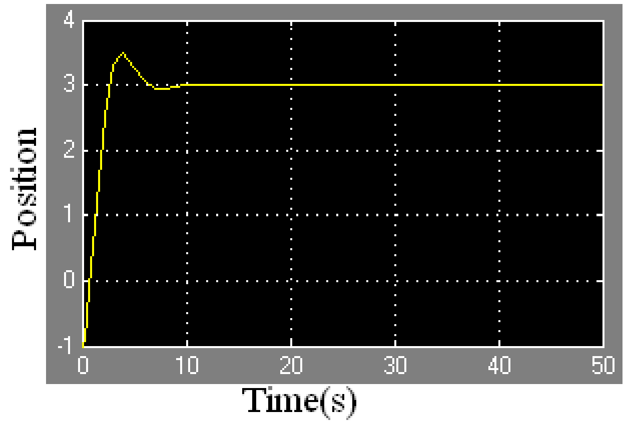


Figure 12. Position of robot controlled by the controller.

When we incorporate a time delay of less than or equal to 0.1s, we can see that the system becomes completely unstable (as shown in the scope output in figure 14). We used equations 15, 17 and 18 to create a simulation in the presence of time delay in the controlled network system as shown in figure 13.

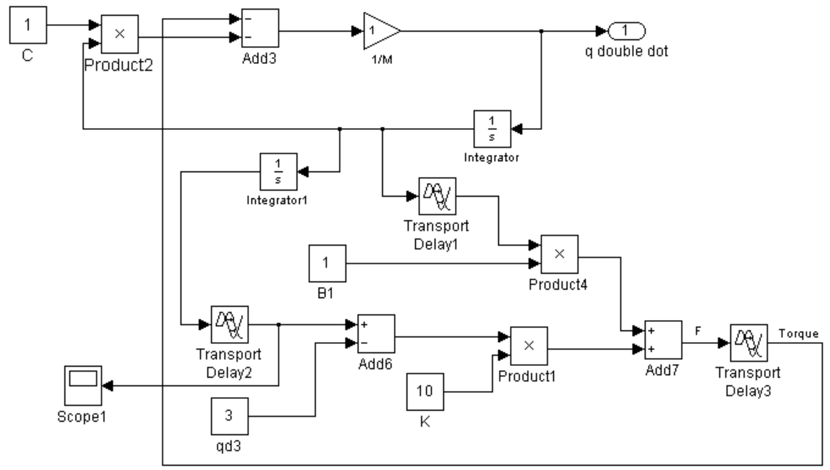


Figure 13. Simulation in the case of time delay using equations 15, 17 and 18.

Figure 14 describes the output of the simulation, in figure 13, when the time delay is 0.1s. The output of the simulation clearly shows the system is unstable for a time delay of less than one millionth of seconds. Hence in the presence of time delay the plant cannot be controlled as desired because the system becomes unstable.

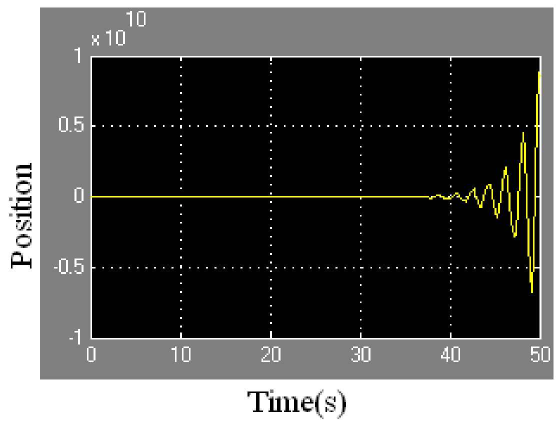


Figure 14. Position of robot when time delay=0.1s.

Using the same wave scattering blocks as we used in the bilateral teleoperation system (described by equation 14 and as shown in figure 3(a) and 3(b)), we can design a simulation (figure 15) to solve the time delay problem in the controlled network system as well.

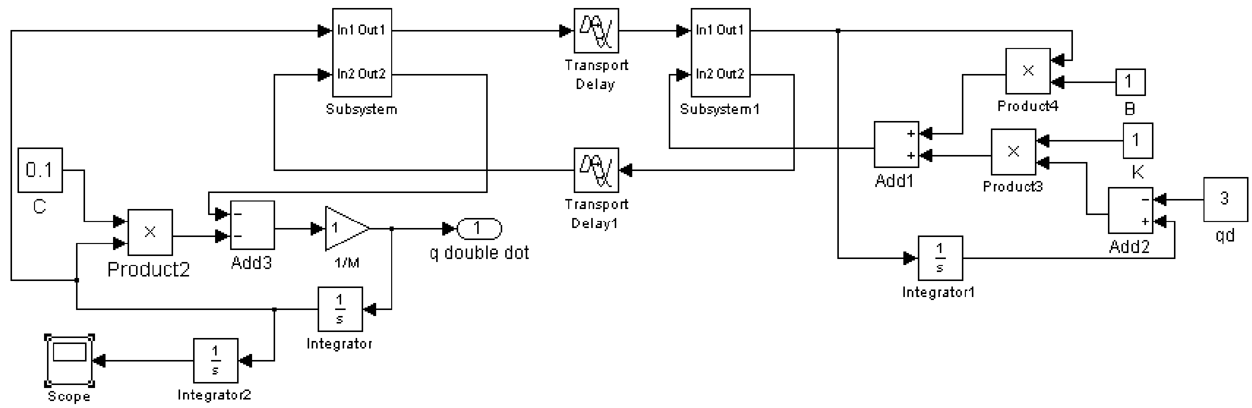


Figure 15(a). Simulation designed for solving time delay problem using wave scattering transformation.

Figure 15(a) can be represented in a simple block diagram as shown in figure 15(b)

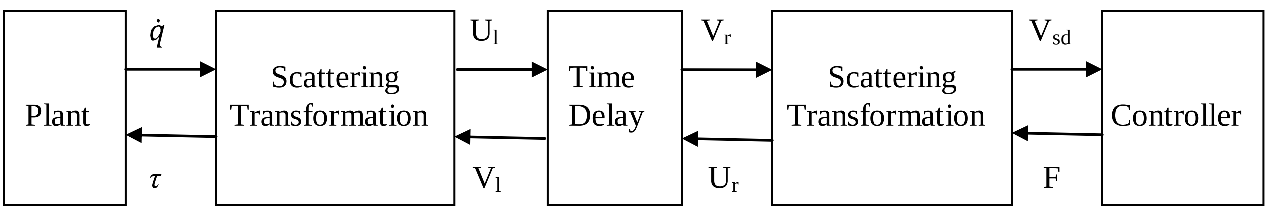


Figure 15(b). Block diagram representation of simulation shown in figure 15(a).

When we look at the scope output of the above simulation we found that the system becomes stable for a delay of 50s or longer. In figure 16, the position of the plant is controlled to 3 units as desired, when the time delay is 0.5s.

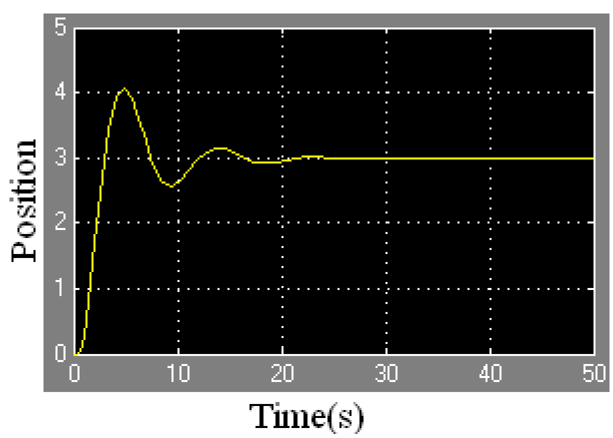


Figure 16. Position of robot controlled as desired when time delay=0.5s and b=1.

Hence, we can conclude that wave scattering equations works for solving the time delay problem in the controlled network system as well.

## Introduction to Servomechanism

The term servomechanism refers to "any feedback control system whose output is the mechanical position of one object relative to another."[8] It can also be referred to as the positional control system. The term feedback control system has a broad meaning because it includes all devices that involve feedback and power amplification whether it is electronic, mechanical or hydraulic.[8] We can see the feedback control being used in our daily lives. Few examples of feedback control are air-conditioning system, automatic washing machine, temperature controls for heating plant, and electronic voltage regulators.[8]

## Servomechanism Experiment for Controlled Network System

Similar to the controlled network system, a servo apparatus consists of a servo plant which is connected to the computer which acts as a controller. Hence we used servomechanism experiment to test our theoretical simulation of controlled network system for all three cases: in absence of time delay, in presence of time delay and in case of time delay compensation.

We set up the apparatus as shown in fig. 17. The servo plant is connected to the computer via a UPM (universal power module) and DAQ (Data acquisition) card. The motor input of the servo plant goes to the load on UPM, and the potentiometer output goes to the S1 or S2 on UPM.[9] Similarly, the tachometer output goes to S3 or S4 on UPM. The UPM provides power to the motor. The potentiometer attached in the servo plant serves as an angle sensor, and the tachometer serves as an angular speed sensor. The three external gears on the servo plant are all with the same radius. The anti-backlash gears, with two internal springs, are set up on the sensors. The two halves of the anti-backlash gear are rotated with respect to each other so that they can load the springs before the gear is meshed with the center gear.[9]

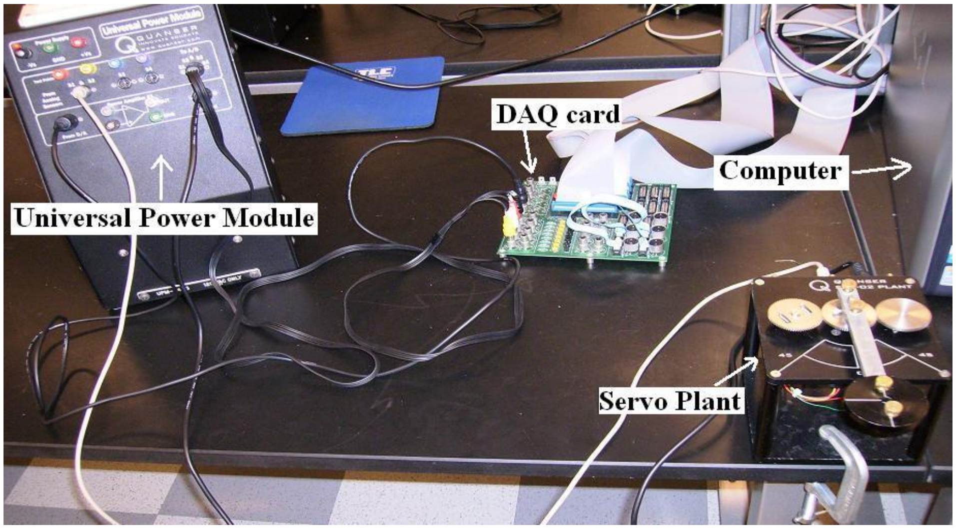


**Figure 17. Experimental set up for controlled network system.**

Before starting the experiment we calibrated the servo apparatus as described in the appendix section. We tried to make the zero angle of the load correspond to the zero angle of the servo.[9]

We built the simulation in MATLAB to control the servo plant as shown in figure 18. The purpose of the Quanser Multi Q-PCI DAC block is to convert the digital signal into analog signal, and it is the input to the system. The purpose of the Quanser Multi Q-PCI ADC block is to convert the analog signal into digital signal, and it is the output from the system. We used the potentiometer's scope to get the position as the output from the system. Since we used the scope to get the feedback for the position, the system was not passive. Hence when we incorporated a small time delay in our servo system, it became completely unstable. The simulation of the servo system is shown in figure 18.

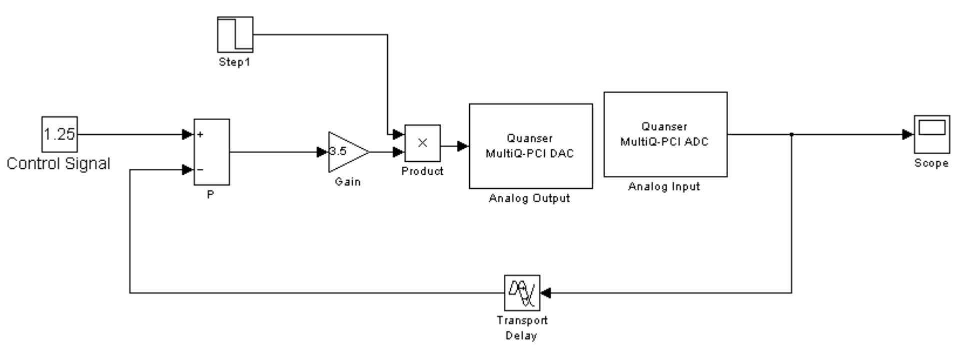


**Figure 18. Simulation when potentiometer's output is used to get position feedback.**

We multiplied the signal going into the Quanser DAC block (input to the system) with a step input for safety precaution. We set the initial value of the step function to 1, step time to 10s and final value to 0. After 10s, the input to the system is zero in order to prevent the DC motor with frightening amounts of energy. We tried setting the time delay to 0.03s in the feedback loop that goes into the controller (figure 18). The servo became very unstable as shown in figure 19.

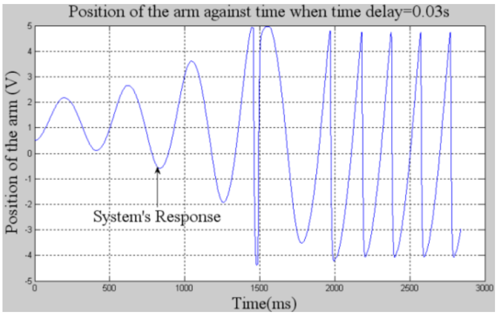


**Figure 19. Unstable system when time delay is 0.03 seconds.**

We also used tachometer to get the velocity feedback from the output. After that, we integrated the velocity feedback to get the position feedback in order to build a PI controller. The simulation using tachometer's output in order to get a velocity feedback is shown in figure 20.

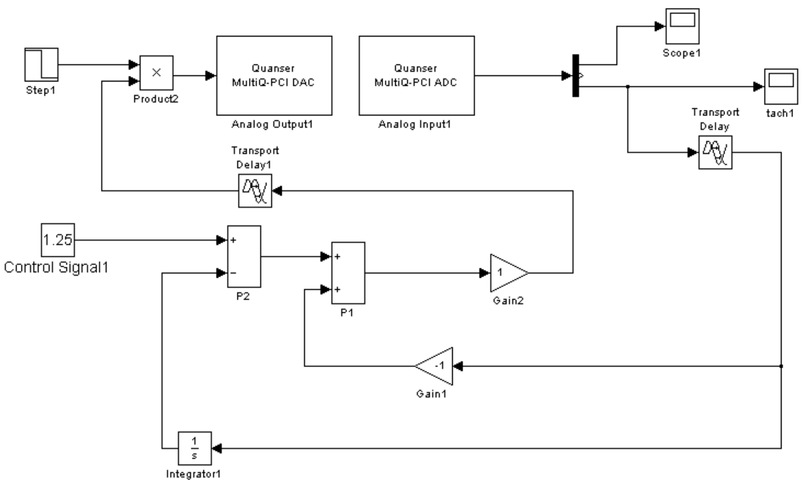


**Figure 20. Simulation when tachometer's output is used to get velocity and position feedback.**

Since we used the tachometer, the system is passive, and it stayed stable until 0.2s and started becoming unstable starting at 0.3s (figure 22). Hence we concluded that the tachometer is 10 times tolerant to time delay compared to the potentiometer. Figure 21 is the output generated by the simulation in figure 20, and it depicts the system goes to the desired position as controlled in the simulation in the absence of time delay. The desired position reached to -1.25 rather than +1.25 because we multiplied the velocity feedback with a gain of -1 as we wanted to build a PI controller.

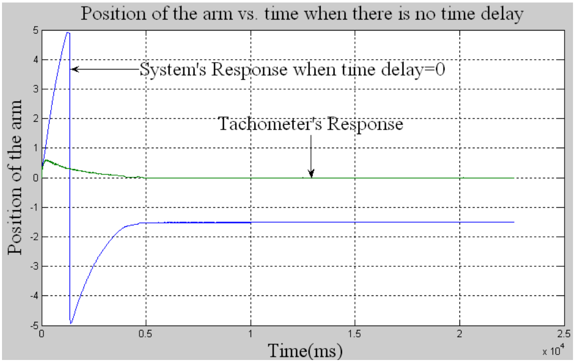


**Figure 21. System's and tachometer's response when there is no time delay in the system.**

As the system's response (blue line) gets constant, the tachometer's response (green line) in figure 21 eventually goes to zero. The position from the system's response is constant after some time and reaches to the desired position. As a result the tachometer's response goes to zero because tachometer gives the velocity feedback, and we know that the derivative of a constant is zero. The steady state error in system's response in figure 21 is 0.268. Figure 22 shows the system becomes completely unstable when we set the time delay to be 0.3s.

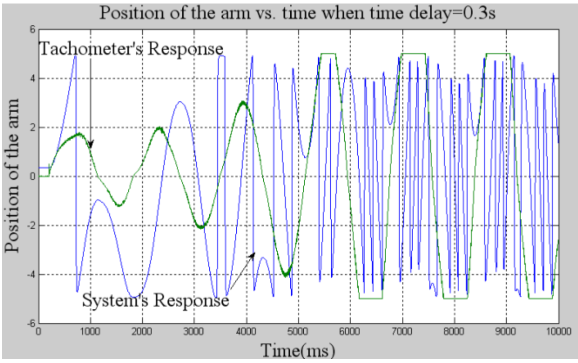


**Figure 22. System's and tachometer's response when time delay =0.3 second.**

Once we found that the system was unstable for small time delay, we tried to make it stable by incorporating the wave scattering transformation as shown in equation 14. We used the scattering transformation from figure 3(a) and 3(b) to solve the time delay problem. The simulation for solving the time delay problem using scattering transformation is shown in figure 23.

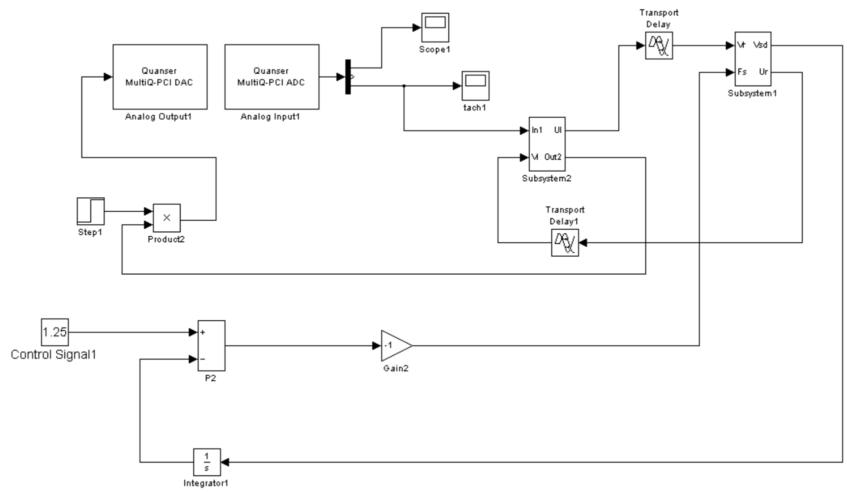


**Figure 23. Simulation in case of wave scattering for solving the time delay.**

Since we are incorporating wave scattering blocks (subsystem 1 and subsystem 2) in our simulation model in figure 23, we made some slight changes to make the system stable and reach to its desired position. We multiplied the controller's position command with a gain of -1 and to overcome this negative gain we substituted -1 instead of 1 for the initial value of the input step function. In wave scattering block, we also substituted $\frac{1}{(b+1)}$ instead of $\frac{1}{b}$ in the gain 4 block (in figure 3b) into our simulation model in figure 23. We came to the conclusion that our practical simulation is consistent with the theoretical simulation because from figure 24 and 25 it is clear that the system becomes stable and the position of the servo arm reaches its desired position. Figure 24 is the output generated by the simulation in figure 23 when time delay is 0.5s and b=1 for the wave scattering transformation.

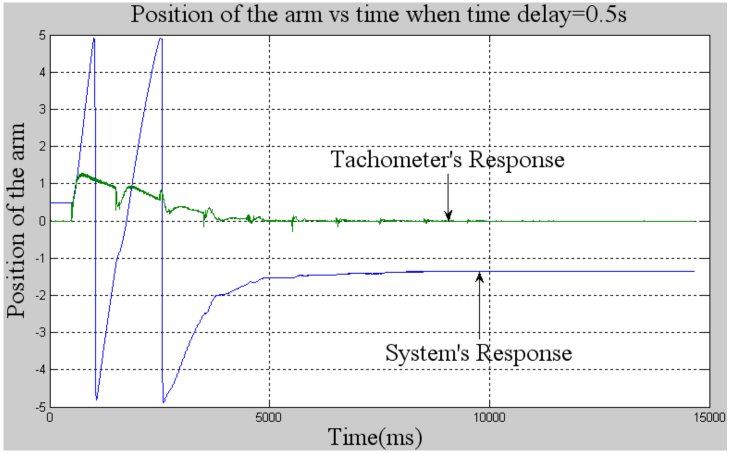


Figure 24. Time delay compensation for controller and plant even when time delay is 0.5s and b=1.

For 0.5s time delay, the steady state error is 0.113. The desired position reached to -1.25 rather than +1.25 because we multiplied the controller's desired position command with a gain of -1 for the purpose to make the system stable as seen in figure 23.

When the time delay is set to 2s the system is still stable (figure 25), but with greater steady state error.

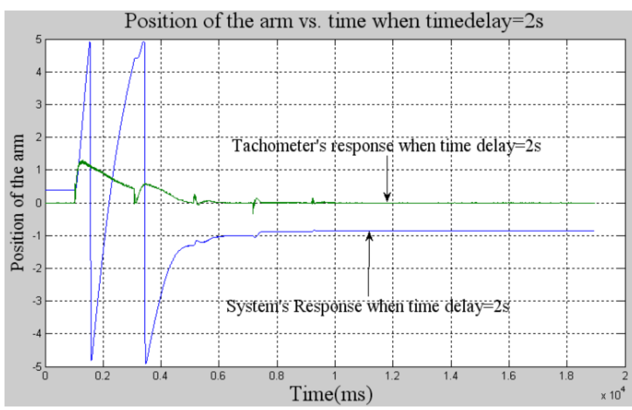


Figure 25. Time delay compensation for controller and plant even when time delay is 2s and b=1.

For 2s time delay, the steady state error is 0.400. Figure 26 shows the position of the servo arm against the time when the time delay is 5s. The steady state error in system's response is 0.466 as shown in figure 26.

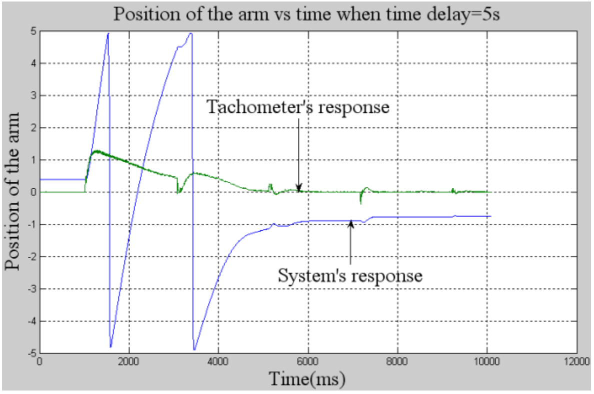


**Figure 26. Time delay compensation for controller and plant even when time delay is 5s and b=1.**

Figure 27 shows the position of the servo arm against the time when the delay is 100s. The steady state error in system's response is 0.569.

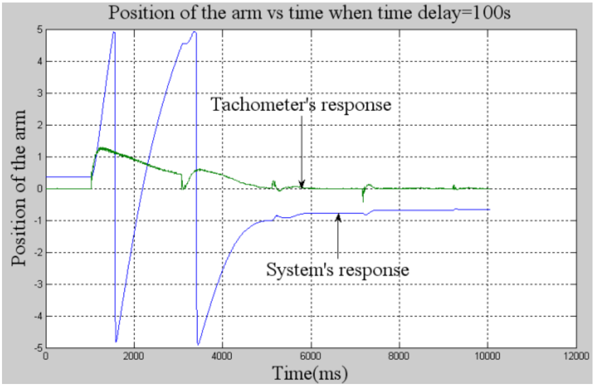


**Figure 27. Time delay compensation for controller and plant even when time delay is 100s and b=1.**

From figures 24, 25, 26 and 27 it is clear that as the time delay increased, the steady state error in system's response increased as well.

At last, we designed a simple P controller to control the servo system. We created a simulation for a simple P controller as shown in figure 28. We designed and implemented our system such that the input voltage of the motor is set to be zero whenever the rotor angle exceeds 130 degrees, which is equivalent to about 4.3 volts (calculated from the linear fit equation given in figure 30 in appendix section). The simulation of P controller is shown in figure 28.

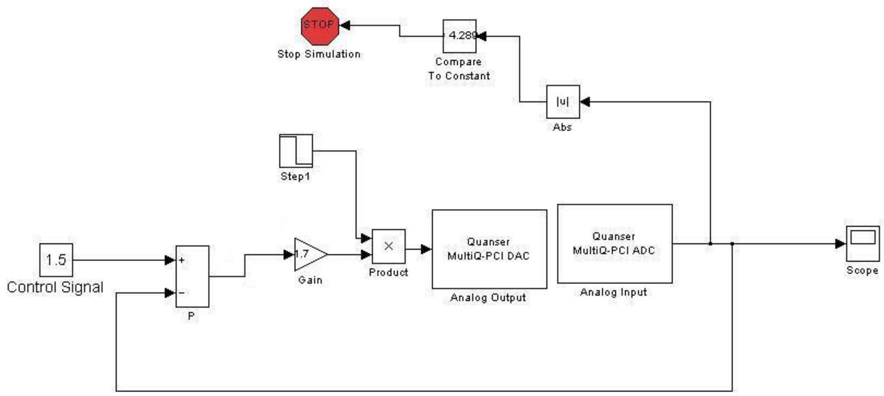


**Figure 28. Figure describing a P controller when potentiometer's output is used to get position feedback.**

Figure 29 shows the output generated by the simulation in figure 28.

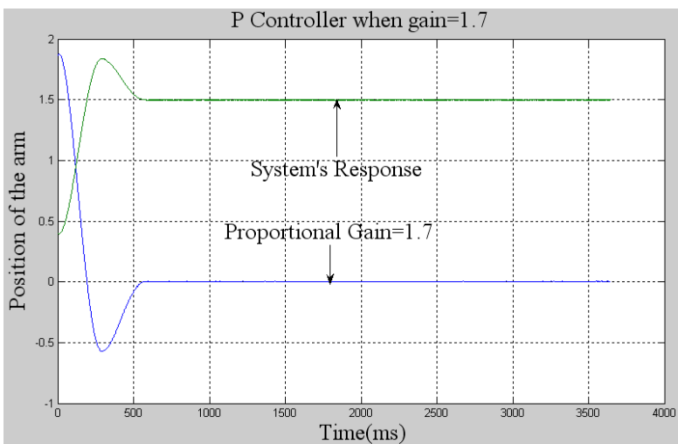


**Figure 29. Figure describing the P controller when gain=1.7.**

We determined the steady state error in system's response for P controller to be 0.002.

## Conclusion

We were able to control mechanical systems over unreliable communication networks in the presence of time delays in communication port. To control bilateral teleoperation and network controlled system (Controller and Plant), we created a theoretical simulation design, in MATLAB, for three cases: in the absence of time delay, in the presence of time delay, and in the case for solving time delay. We noticed that in bilateral teleoperation and controlled network systems, a time delay of less than one millionth of seconds made the system completely unstable. To overcome this problem, we used the wave scattering transformation, as described in equation 14, to build a block shown in fig 3(a) and 3(b). We incorporated these two wave scattering blocks in our theoretical simulation of time delay. The bilateral teleoperation system became completely stable and remained stable for delay of about 2s or less. The controlled network system also remained stable and reached the desired position for delay of about 50s or more. Hence, we concluded that the wave scattering equations worked for solving the time delay problem in the controlled network system as well. We tested the theoretical simulation of controlled system network on simple servo system for three cases: in the absence of time delay, in the presence of time delay, and in the case of solving time delay. When there was no time delay, the system was controlled to its desired position with a steady state error of 0.268 in system's response. We incorporated a time delay of 0.03s in the position feedback provided by the potentiometer. The system was completely unstable. Similarly, we tried a time delay value of less than or equal to 0.2s, in the velocity feedback provided by the tachometer. We noticed that the system was stable for the value less than or equal to 0.2s. However, the system became unstable for the time delay of 0.3s. We concluded that since the tachometer is a passive system, it can tolerate ten times greater time delay than the potentiometer can. We can say that a passive system improves the performance of the system. In lab, we implemented the same scattering wave transformation blocks (fig 3a and 3b) to solve the time delay problem in our servo system. We tried the values of time delay up to 100s and the system became stable. Hence we concluded that the practical system is completely stable even for higher values of time delay. However, we found that as the time delay increased, the steady state error increased as shown in figures 24, 25, 26 and 27. For time delay of 0.5s, 2s, 5s and 100s, the steady state error was 0.113, 0.400, 0.466

and 0.569 respectively. We believe that the reason for the steady state error is due to the calibration of the tachometer. We didn't calibrate the tachometer in our system because the response from the tachometer was noisy. We also built a simple P controller and determined its steady state error in system's response to be 0.002 for the proportional gain of 1.7.

# Appendix

## Calibration of Potentiometer

The motor input and the sensor output of the potentiometer are in volts, but the voltages do not correspond to the same angles. [9] Hence it is important to calibrate the potentiometer. In order to calibrate the potentiometer we detached the wire from the load on UPM (universal power module) so that we can attach a display (from Simulink library) to the output in our simulation model shown in figure 28. Since now the motor does not have a power, we moved the servo arm to 0, $+45^0$ and $-45^0$ and the display attached in the simulation gave us the corresponding voltage outputs as shown in table 1.

| Angle | Voltage output from Potentiometer |
|---|---|
| $+45^0$ | 1.83 |
| 0 | 0.48 |
| $-45^0$ | -0.79 |

**Table 1. Table showing angle of servo arm with its corresponding voltage outputs.**

We plotted the angle against the voltage in Excel as shown in figure 30. The linear fit result of the plot gave us a relation between the angle of the servo arm and the voltage output from the potentiometer.

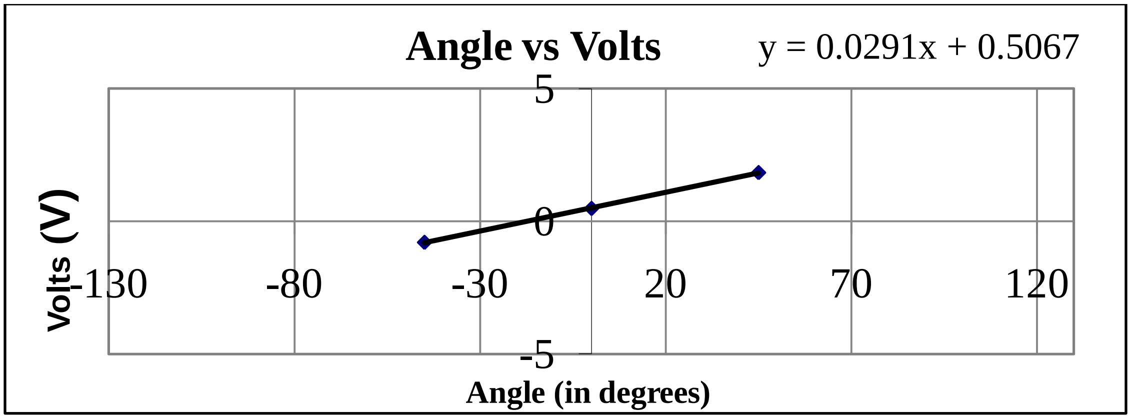


Figure 30. Angle of the servo arm vs. the voltage output from potentiometer.

## Nomenclature and different components of servo plant

The three different views of servo plant are shown in figures 31, 32 and 33.[11] Figures 31, 32 and 33 show the view from front, view from under the top plate and view from back of the servo plant respectively.

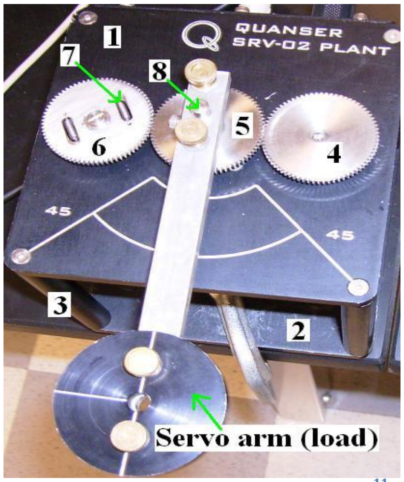


Figure 31. Front view of servo plant.[11]

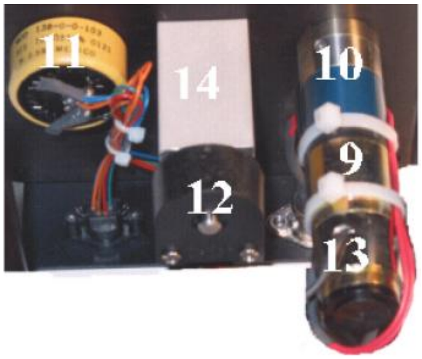


Figure 32. Servo plant view under the top plate.[11]

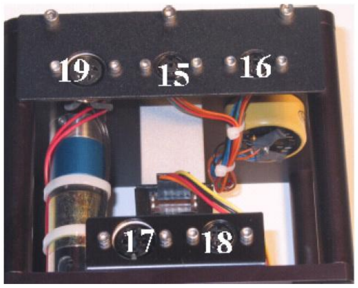


Figure 33. Connection view from the back of the servo plant.[11]

The name of the components shown in figures 31, 32 and 33 are described in table 2 as given by the servo user manual.[11]

| | | | |
|---|---|---|---|
| 1 | Top Plate | 11 | Potentiometer |
| 2 | Bottom Plate | 12 | Encoder |
| 3 | Posts | 13 | Tachometer |
| 4 | Standard Motor Gear | 14 | Bearing Block |
| 5 | Output Gear | 15 | Potentiometer Connector |
| 6 | Potentiometer Anti-Backslash Gear | 16 | S2 Connector |
| 7 | Anti- Backslash Springs | 17 | Encoder Connector |
| 8 | Output Shaft/ Load Shaft | 18 | Tachometer Connector |
| 9 | Motor | 19 | Motor Connector |
| 10 | Gearbox | | |

**Table 2. Table showing different components of the servo plant from figures 31, 32 and 33.**

## Acknowledgement

I would like to express my gratitude to Dr. Nikhil Chopra for his mentorship and guidance throughout the 10 weeks of the research. I would like to thank the controls lab coordinator, Jay Renner, and the graduate student in the bilateral teleoperation lab, Yenchen Liu, who helped me in the labs during my research. I would also like to thank the Institute for Systems Research at the University of Maryland for providing me with this wonderful research opportunity. Finally, I want to thank to the National Science Foundation (NSF) for providing the generous funding that made this research possible for me.

## Bibliography

1) G. Niemeyer and J. E. Slotine, “Stable Adaptive Teleoperation” IEEE Journal of Oceanic Engineering, Volume 16, no. 1, January 1991.

2) R. J. Anderson and M.W. Spong, “Bilateral Control of Teleoperators with Time Delay,” IEEE transactions on automatic control, Volume 34, no. 5, May 1989.

3) Peter F. Hokayem and Mark W. Spong, “Bilateral Teleoperation: An Historical Survey,” Automatica, Volume 42, Issue 12, Pages 2035-2057, December 2006.

4) M. W. Spong, S. Hutchinson and M. Vidyasagar, “Robot Modeling and Control,” NJ, John Wiley and Sons, Inc. 2006.

5) B. D. O. Anderson and S. Vongpanitlerd, “Network Analysis and Synthesis,” New York, Dover Publications, Inc., 2006.

6) F. L. Lewis, C.T. Abdallah and D.M. Dawson. “Control of Robot Manipulators,” New York, Macmillan publication company, 1993.

7) William J. Palm III, "System Dynamics," New York, Mc Graw Hill Higher Education, 2005.

8) Newton Jr., G.C., Gould, L. A., and Kaiser, J.F. (1957). “Analytical Design of Linear Feedback Controls,” John Wiley and Sons.

9) W. S. Levine, S. Bergbreiter and J. Renner. “Control Laboratory 3: Simple Servomechanism Experiment.” March 2008.

10) Bahram Shahian and Michael Hassul, “Control System Design Using MATLAB,” Princeton Hall, NJ 1993

11) “SRV02-Series Rotary Servo Plant user manual,” August 5, 2008, Quanser, <http://www.fer.hr/_download/repository/SRV02_User_Manual.pdf>